NOVEL FITTING METHOD OF FORMING TOOL PROFILE IN PRECISION GRINDING SCREW ROTOR

Zhihuang SHEN[1]

In rotor research, obtaining a smooth screw rotor profile is essential. However, current studies have not developed a precise fitting method to smoothen forming tool profiles. Hence, a fitting processing method based on a wavelet smoothing theory and parameter cubic spline interpolation is proposed. The wavelet smoothing method removes high frequency parts of the forming tool profile curvature and smoothens bad points. Parameter cubic spline interpolates the larger distance of the point set of the forming tool profile. These results demonstrate that wavelet smoothing and parameter cubic spline interpolation can help calculate the smooth grinding profile of the screw rotor.

Keywords: Screw rotor, Forming tool, Fitting, Wavelet, Parameter Cubic Spline.

1. Introduction

Screw rotors with complex helical profiles have been widely used in positive displacement screw machines, such as screw pumps, screw compressors, screw vacuum pumps, and screw expanders [1]. A pair of conjugate screw rotors is the most crucial component of the twin-screw compressor, whereby the machining precision of the screw rotors can considerably affect the performance of the compressor. In recent years, screw rotors are being machined primarily by grinding or milling methods. Hence, calculating the screw rotor profile or forming tool is a critical problem for rotor research. Litvin [2] applied the enveloping method proposed by Euler in the eighteenth century to design and manufacture gears. Xing [3] used the concept of a gearing envelope theory to establish the equation of the contact line between the screw rotor and the forming tool and calculated the forming tool profile from the rotor profile. Liu [4] investigated the influence of installation angle, center distance, and grinding wheel wear on rotor profile error. Moreover, he proposed a novel method for precisely predicting profile error of the screw rotor from grinding. Li [5] proposed a novel calculation process based on the groove machining principle to compute the wheel profile with known groove model and wheel axis setting conditions. The relationship between motion parameters and profile error of screw rotor was also simulated. Zhao [6,7] conducted considerable research on form grinding of screw rotor,

[1] PhD, College of Mechanical and Energy Engineering, Jimei University, China, e-mail: shenzhihuang@jmu.edu.cn

which involved precision grinding of screw rotors using the computer numeral control (CNC) method. In 2012, Wu [8] suggested a design method of forming tool profiles for machining rotors with the aid of an arbitrary rotor profile (either analytical or discrete forms of rotor profile). In the above-cited studies, the mathematical model of analytic gearing envelope method was sufficiently accurate. However, computing the nonlinear equation of contact line proved to be very challenging with the current mathematical models. The calculation process of the nonlinear equation was tedious, making it difficult to obtain the correct value. This resulted in the generation of bad points and uneven distribution of forming tool profile. Therefore, several scholars have aimed their studies to determine a precise fitting method to smooth the forming tool profile.

Liu [9] studied a concrete algorithm of reconstruction matrix in the process of multi-resolution fairing for curves with arbitrary number of control vertexes. Zarmehi [10] presented the primal and dual matched multiple knot B-spline scaling and wavelet functions whose main properties of smoothness and bi-orthogonality were retained. Jiang [11] promoted an algorithm to the cubic B-Spline curve approximate fields which is based on the double quadratic B-Spline curves. Zhao [12] presented a new immune genetic algorithm (IGA) for point cloud fitting that fits a noisy 3D-point cloud using a B-spline surface with approximate G1 continuity. Wu [13] used cubic splines to fit discrete point data of the screw rotor profile with clearance and produce the grinding wheel profile. Although the above investigations all concentrated on fairing of curves or fitting discrete point data of the screw rotor profile in detail, the control method of the forming tool profile was never investigated.

In the present study, the calculation process of the forming tool profile from the screw rotor is established, for improving the machining precision of the screw rotor. To address the bad points and the uneven distribution of the forming tool profile generated by the analytic gearing envelope method of screw rotor, a fitting processing method of the forming tool profile is proposed. This is based on the theory of the wavelet smoothing and the parameter cubic spline interpolation. The wavelet smoothing method is used to remove the high frequency part of the forming tool profile curve and to smooth the bad points of the forming tool profile with the remaining low frequency part. Cubic spline is used to interpolate the larger distance of the point set of the forming tool profile. Finally, a machining test of the screw rotor is conducted to verify the accuracy of the fitting theory to the forming tool profile.

2. Calculation of the forming tool profile

As is shown in Fig. 1, a coordinate system of the forming tool machining for screw rotor is presented. The coordinate system S_r is attached to the rotor,

rotating around the z_r -axis, while the coordinate system S_g is fixed to the forming tool, rotating around the z_g -axis. The center distance a is defined as the minimum distance between the z_r -axis and the z_g -axis, and Σ is the shaft angle between two axes. The coordinate transformation from S_r to S_g can be derived as :

$$\boldsymbol{M} = \begin{bmatrix} 1 & 0 & 0 & -a \\ 0 & \cos\Sigma & -\sin\Sigma & 0 \\ 0 & \sin\Sigma & \cos\Sigma & 0 \\ 0 & 0 & 0 & 0 \end{bmatrix} \tag{1}$$

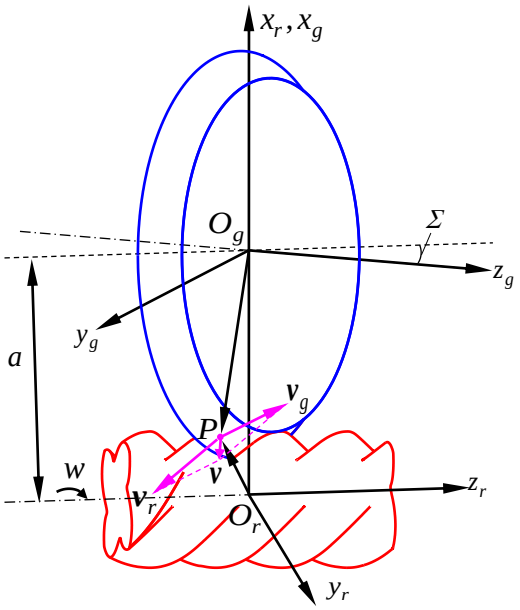

Fig. 1. Coordinate system between screw rotor and forming tool

The rotor profiles are usually expressed in the discrete form, assuming the coordinates of the discrete points, $P = \{(x_i, y_i), i = 1,2,...,n\}$, and the equation of rotor profile can be obtained as follows:

$$\boldsymbol{r}_0 = [x(s), y(s)] \tag{2}$$

where s is the accumulated chord length parameter.

The helicoids of the rotors can be expressed by the following equation:

$$\boldsymbol{r}(s,\theta) = [x, y, z] = [x(s)\cos\theta - ey(s)\sin\theta, ex(s)\sin\theta + y(s)\cos\theta, p\theta] \tag{3}$$

where $e = 1$ for the right-hand rotor， $e = -1$ for the left-hand rotor, θ is the rotation angle of the rotor, and $p = Pz/2\pi$ is the helix parameter, which means that the rotor translates a distance of lead Pz when it rotates one turn. The partial derivatives of the helicoids of the rotor can be calculated by the equation (3):

$$\begin{cases} \boldsymbol{r}_S = \left[\dfrac{\partial x(s)}{\partial s}\cos\theta - e\dfrac{\partial y(s)}{\partial s}\sin\theta, e\dfrac{\partial x(s)}{\partial s}\sin\theta + \dfrac{\partial y(s)}{\partial s}\cos\theta, 0 \right] \\ \boldsymbol{r}_\theta = \left[-x(s)\sin\theta - ey(s)\cos\theta, ex(s)\cos\theta - y(s)\sin\theta, p \right] \end{cases} \tag{4}$$

The normal vector of the helicoids of the rotor can be presented as:

$$\boldsymbol{n} = [n_x, n_y, n_z] = (\boldsymbol{r}_S \times \boldsymbol{r}_\theta)^T = \begin{bmatrix} p\left(e\dfrac{\partial x(s)}{\partial s}\sin\theta + \dfrac{\partial y(s)}{\partial s}\cos\theta \right) \\ p\left(-\dfrac{\partial x(s)}{\partial s}\cos\theta + e\dfrac{\partial y(s)}{\partial s}\sin\theta \right) \\ e\left(x(s)\dfrac{\partial x(s)}{\partial s} + y(s)\dfrac{\partial y(s)}{\partial s} \right) \end{bmatrix}^T \tag{5}$$

According to envelope principle, the relative velocity $\boldsymbol{v}$ between the rotors and the forming tools can be calculated as:

$$\boldsymbol{v} = [v_x, v_y, v_z] = [y\cos\Sigma + z\sin\Sigma, (x-a)\cos\Sigma, (x-a)\sin\Sigma] \tag{6}$$

To determine the relationship equation between the profile parameter s and the rotational angle θ. According to the envelop principle, the contacting condition between screw rotor and forming tool is that the common normal vector $\boldsymbol{n}$ at the contact point is perpendicular to the relative velocity $\boldsymbol{v}$ direction, and can be shown below:

$$\begin{aligned} &\boldsymbol{v}\cdot\boldsymbol{n} \\ &= -p\cos\Sigma\left[ex(s)\sin\theta + y(s)\cos\theta\right]\left[e\frac{\partial x(s)}{\partial s}\sin\theta + \frac{\partial y(s)}{\partial s}\cos\theta \right] \\ &- p\cos\Sigma\left[x(s)\cos\theta - ey(s)\sin\theta - a\right]\left[\frac{\partial x(s)}{\partial s}\cos\theta - e\frac{\partial y(s)}{\partial s}\sin\theta \right] \\ &+ e\sin\Sigma\left[x(s)\cos\theta - ey(s)\sin\theta - a\right]\left[x(s)\frac{\partial x(s)}{\partial s} + y(s)\frac{\partial y(s)}{\partial s} \right] \\ &- p^2\theta\sin\Sigma\left[e\frac{\partial x(s)}{\partial s}\sin\theta + \frac{\partial y(s)}{\partial s}\cos\theta \right] \\ &= 0 \end{aligned} \tag{7}$$

Substituting Eq. (7) into Eq. (3) yields the equation of the contact line:

$$\begin{aligned} &\boldsymbol{r}_{cr} = [x_{cr}, y_{cr}, z_{cr}] \\ &= \left[x(s)\cos f(s) - ey(s)\sin f(s), ex(s)\sin f(s) + y(s)\cos f(s), pf(s)\right] \end{aligned} \tag{8}$$

Then, transforming the equation of contact line $\boldsymbol{r}_{cr}$ from rotor coordinate system S_r to forming tool coordinate system S_g yields:

$$\begin{aligned} \boldsymbol{r}_{cg}^{T} &= \boldsymbol{M}\boldsymbol{r}_{cr}^{T} \\ &= \begin{bmatrix} x(s)\cos f(s) - ey(s)\sin f(s) - a \\ [ex(s)\sin f(s) + y(s)\cos f(s)]\cos\Sigma - pf(s)\sin\Sigma \\ [ex(s)\sin f(s) + y(s)\cos f(s)]\sin\Sigma + pf(s)\cos\Sigma \end{bmatrix} \end{aligned} \tag{9}$$

The contour surface of the forming tool can be generated by rotating the contact line around its rotating axis, and the equation of forming tool can be presented as follows [14,15]:

$$\boldsymbol{r}_g = [Z_g, R_g] = [z_{cg}, \sqrt{x_{cg}^2 + y_{cg}^2}] \tag{10}$$

3 Fitting method of the forming tool profile

The traditional gear meshing principle is accurate when calculating the profile of forming tools. However, the singularity, overcut, or double envelope of the rotor profile result in numerical divergence in the solution of the tool profile. Moreover, the calculated tool profile generates the phenomenon of data oscillations (bad points) and uneven distribution. Therefore, it is necessary to deal with these phenomena pertaining to forming tool profile.

3.1 Unusual phenomenon of the forming tool profile

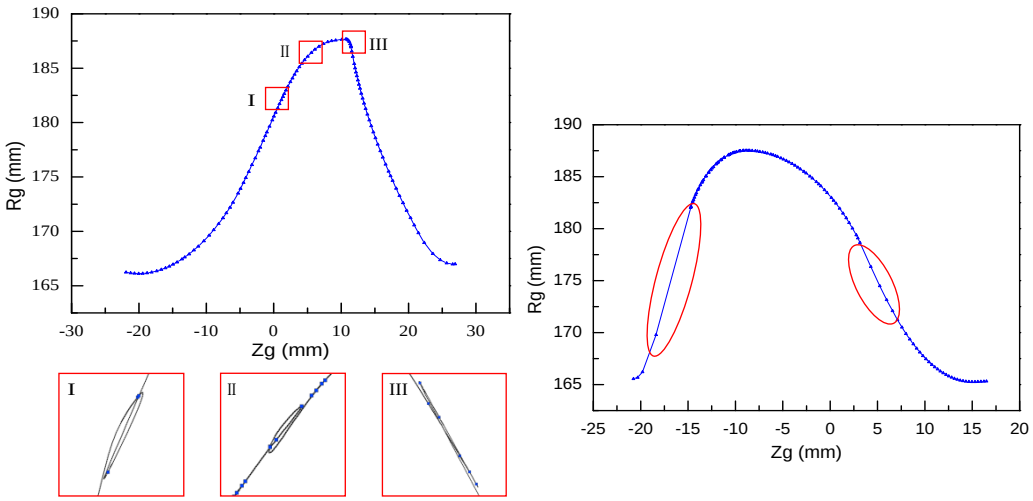

(a) Bad points (b) Unevenly distributed points

Fig. 2. Unusual phenomenon of the forming tool profile

Fig. 2 shows the unusual phenomenon of the forming tool profile. Fig. 2(a) shows a considerable number of bad points in the forming tool profile. Fig. 2(b) shows that the forming tool profile points are unevenly distributed seen as a large span interruption. Therefore, it is necessary to fit the calculated forming tool profile.

3.2 Wavelet method to eliminate bad points

Common smoothing methods for the elimination of bad points include energy method, least square method, rebound method, base spline method, round rate method and wavelet smoothing method. According to the signal processing theory, the initial curvature of the forming profile curve can be divided into two parts. The first part is the gradual low-frequency part of the curvature signal of the curve, which reflects the true trend of the curvature change. The second part is the high frequency part generated either by measurement error or calculation error.
The wavelet smoothing method primarily uses the multi-resolution characteristic of wavelet representation, and discards or suppresses the high-frequency part to remove the noise signal. Furthermore, it extracts the low-frequency part to obtain a stable signal diagram. Therefore, the wavelet smoothing method is used to smooth the forming tool profile. The profile smoothing steps are as follows:

(1) Calculation of initial curvature curve

The data set of the forming tool profile are $P = \{(R_{gi}, Z_{gi})\big|_{p_i}, i = 1,2,...,n\}$.

Then, the set is reparametrized by the accumulated chord length method (chord length $l_i = |p_i - p_{i-1}|$). The first derivative and the second derivative can be calculated using Eqs. (11) and (12), respectively, as follows:

$$T_i = \frac{dp}{ds}(s_i) = (\dot{x}(s_i), \dot{y}(s_i)) \approx \frac{p_{i+1} - p_i}{l_{i+1}} \tag{11}$$

$$W_i = \frac{d^2 p}{ds^2}(s_i) = (\ddot{x}(s_i), \ddot{y}(s_i)) \approx \frac{2}{l_i + l_{i+1}} \left(\frac{p_{i+1} - p_i}{l_{i+1}} - \frac{p_i - p_{i-1}}{l_i} \right) \tag{12}$$

Substituting Eqs. (11) and (12) into the formula of the plane curve relative curvature, and the relative curvature value can be obtained as follows:

$$k_i = \frac{\dot{x}(s_i)\ddot{y}(s_i) - \ddot{x}(s_i)\dot{y}(s_i)}{\left[\dot{x}^2(s_i) + \dot{y}^2(s_i)\right]^{\frac{3}{2}}} \tag{13}$$

Fig. 3 shows the initial curvature of the forming tool. The high-frequency curvature occurs between points 170–230. The fluctuation of curvature is relatively large, and the maximum value is 27 (point 206).

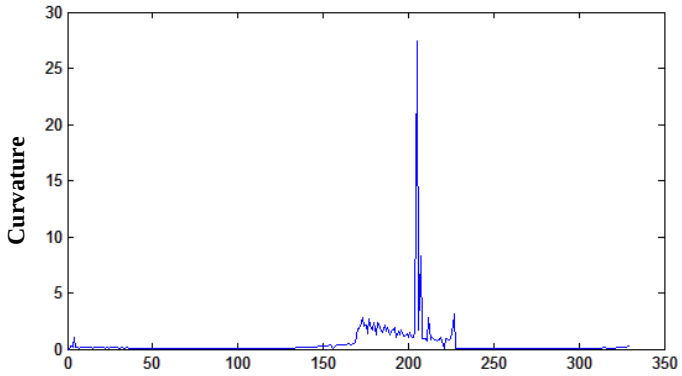

Fig. 3. Initial curvature curve of forming tool

(2) Wavelet decomposition of the initial curvature curve

Fig. 4 shows the low-frequency portion of the initial curvature of the curve as decomposed by the Coiflet wavelet. After decomposition, the high frequency part near point 206 is discarded, the curvature value is controlled at approximately 2.6.

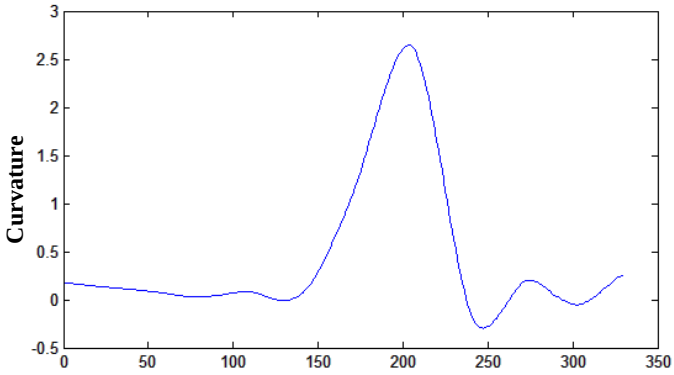

Fig. 4. Low frequency part of the initial curvature of the curve.

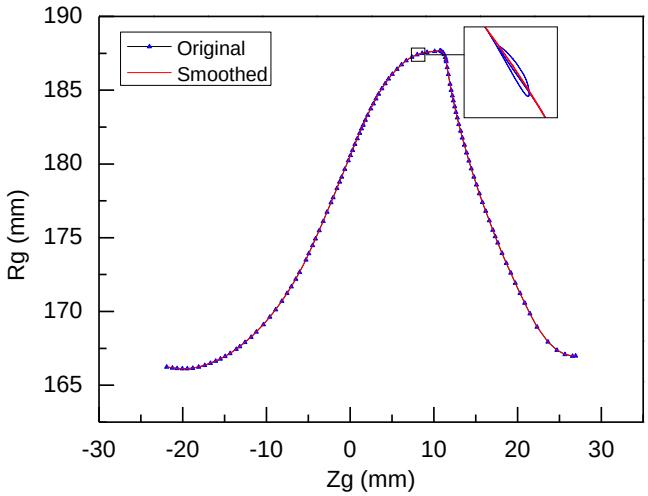

Fig. 5. Comparison of forming tool profile before and after smoothing

According to the low-frequency portion of the forming tool profile initial curvature, the original forming tool profile can be smoothed. The smoothed tool profile and the original tool profile are compared in Fig. 5. The bad points of the forming tool profile are eliminated, and the resulting overall profile of the forming tool is smooth and stable.

3.3 Parameter Cubic Spline Interpolation for the Uneven Distribution of Points

The parameter cubic spline interpolation method is utilized to resolve the uneven distribution of the forming tool profile. The specific interpolation steps are as follows:

(1) The data set of the forming tool profile $P_i(x_i, y_i)$, $i = 0,1,...,n$ are input;

(2) The set is reparametrized using the accumulated chord length method s_i, $i = 0,1,...,n$;

(3) m-continuity equations are established;

(4) The supplementary equation by the given endpoint condition is determined;

(5) Linear equations are calculated using the chase method;

(6) The i-th curve equation of the parameter cubic spline is established as follows:

$$\begin{cases} x_i(s) = \begin{bmatrix} 1 & u & u^2 & u^3 \end{bmatrix} \begin{bmatrix} 1 & 0 & 0 & 0 \\ 0 & 0 & 1 & 0 \\ -3 & 3 & -2 & -1 \\ 2 & -2 & 1 & 1 \end{bmatrix} \begin{bmatrix} x_{i-1} \\ x_i \\ h_i m_{i-1} \\ h_i m_i \end{bmatrix} \\ y_i(s) = \begin{bmatrix} 1 & u & u^2 & u^3 \end{bmatrix} \begin{bmatrix} 1 & 0 & 0 & 0 \\ 0 & 0 & 1 & 0 \\ -3 & 3 & -2 & -1 \\ 2 & -2 & 1 & 1 \end{bmatrix} \begin{bmatrix} y_{i-1} \\ y_i \\ h_i n_{i-1} \\ h_i n_i \end{bmatrix} \end{cases} \tag{14}$$

where $i = 1,2,...,n$, $h_i = s_i - s_{i-1}$, $u = \dfrac{s - s_{i-1}}{s_i - s_{i-1}} = \dfrac{s - s_{i-1}}{h_i}$, $u \in [0,1]$. Parameters m_{i-1}, m_i are the first derivatives of $x_i(s)$, and parameters n_{i-1}, n_i are the first derivatives of $y_i(s)$.

The forming tool profile before and after interpolation is compared in Fig .6, and as shown, the forming tool profile after interpolation is evenly distributed.

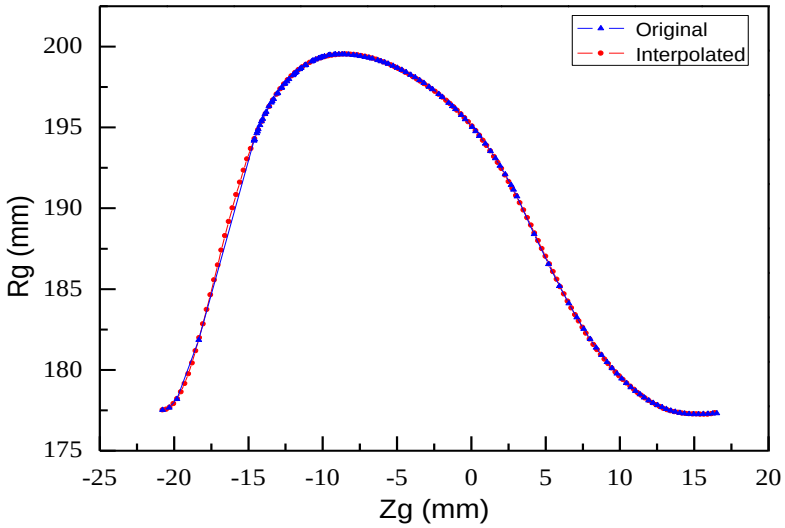

Fig. 6. Comparison of forming tool profile before and after interpolation

4 Example

To verify the correctness of fitting process of the forming tool profile, a pair of rotors are respectively machined by the original and fitted forming tools. The rotors' parameters are listed in Table 1.

Table 1

Parameters of the rotor

Type	Revolving direction	Number of Teeth	Outer Diameter (mm)	Root Diameter (mm)	Lead (mm)	Helical Angle (deg)	Material
Male	Right	4	68.25	39.7635	128	45	42CrMo
Female	Left	5	54.653	27.248	160		

Fig. 7 shows the machining of rotors. To determine the precision of the rotor profile, the end face of rotor is measured using a 3D coordinate measuring machine (CMM), as is shown in Fig. 8.

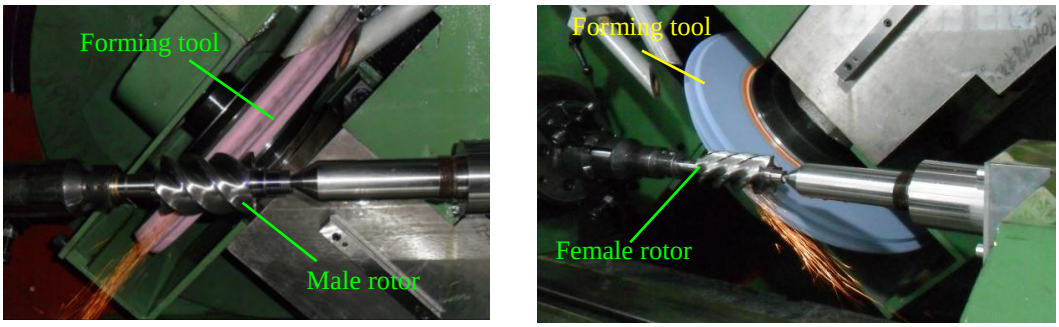

(a) Male rotor (b) Female rotor

Fig.7. Machining of rotors

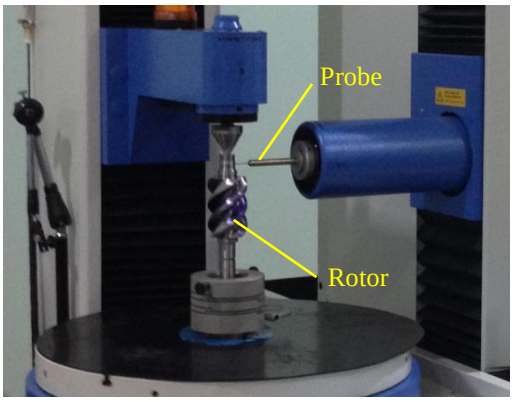

Fig. 8. Measurement of rotors

Fig. 9(a) shows that the maximum normal error of the rotor profile points machined by the not-smooth forming tool is 0.0145 mm(Region A). The normal errors of Region A are mainly caused by the bad points. The normal error of. Further, the rotor profile normal error machined by the smoothed forming tool profile can be controlled in the range of -0.01 mm to 0.01 mm. Fig. 9(b) shows that the normal error of the rotor profile points machined by the uninterpolated forming tool is 0.0124 mm(Region B), and the normal error is slightly larger than the interpolated forming tool. The normal errors of Region B are mainly caused by the unevenly distributed points.

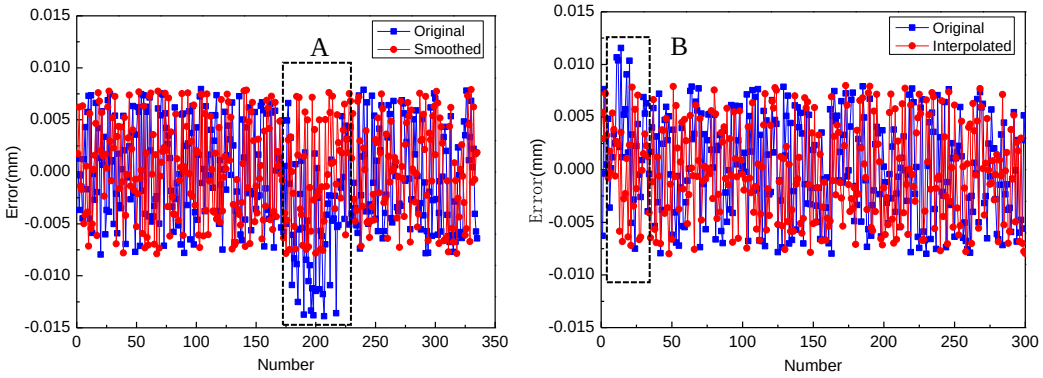

(a) Normal error of male rotor profile points (b) Normal error of female rotor profile points

Fig. 9. Comparison of profile error of rotors

5 Conclusions

This paper presents a fitting processing method of the forming tool profile that is based on the theory of the wavelet smoothing and where the parameter cubic spline interpolation is proposed. The wavelet smoothing method is employed to remove the high frequency part of the forming tool profile curvature curve, smoothing the bad points of the forming tool profile with the remaining

low frequency part. The parameter cubic spline is utilized to interpolate the large distance of the point set of the forming tool profile.

The numerical examples demonstrate that the maximum normal error of the rotor profile points machined by the not-smooth forming tool is 0.0145 mm, and the maximum normal error of the rotor profile points machined by the uninterpolated forming tool is 0.0124 mm. The rotor profile normal error machined by the smoothed or uninterpolated forming tool profile all can be controlled in the range of -0.01–0.01 mm. These results demonstrated that the fitting method based on the theory of the wavelet smoothing and the parameter cubic spline interpolation effectively helped calculate the grinding profile of the screw rotor or the forming tool.

Acknowledgement

This work was financially supported by the Science and Technology Project of Fujian Province, China (Project No. 2018J05087), and the Science and Technology Department Project of Fujian (Project No. JK2017025).

R E F E R E N C E S

[1]. *Kovacevic A, Stosic N, Mujic E, et al,* CFD integrated design of screw compressors[J], Engineering Applications of Computational Fluid Mechanics, **vol**. 1, no. 2, Feb. 2007, pp. 96-108.

[2]. *F.L. Litvin,* Theory of Gearing[M], second ed, 1968, Nauka, Moscow, 1956.

[3]. *Xing ZW,* Screw Compressors: Theory, Design and Application[M], Beijing: Machine Press, 2000. (in Chinese).

[4]. *Liu Z, Tang Q, Liu N, et al,* A profile error compensation method in precision grinding of screw rotors[J], The International Journal of Advanced Manufacturing Technology, **vol**. 100, no. 9-12, Feb. 2019, pp. 2557-2567.

[5]. *Li G,* A new algorithm to solve the grinding wheel profile for end mill groove machining[J], The International Journal of Advanced Manufacturing Technology, **vol**. 90, no. 1-4, Apr. 2017, pp. 775-784.

[6]. *Zhao Y, Zhao S, Wei W, et al,* Precision grinding of screw rotors using CNC method[J], The International Journal of Advanced Manufacturing Technology, **vol**. 89, no. 9-12, Apr. 2017, pp. 2967-2979.

[7]. *Zhao Y, Zhao S, Hou H, et al,* Determining the repair width and CNC grinding of screws of triple-screw pump[J], The International Journal of Advanced Manufacturing Technology, **vol**. 97, no.1-4, July 2018, pp. 389-400.

[8]. *Wu B H, Zhang J, Yang J H, et al,* Calculation Method for Edge Shape of Forming Wheel for Screw Rotors Machining[J], Journal of mechanical engineering, **vol**. 48, no. 19, Oct. 2012, pp. 192-198. (In Chinese)

[9]. *Liu DP, Ji XG, et al,* Rapid Wavelet Construction of Multi-resolution Fairing for Curves With Arbitrary Number of Control Vertexes[J], Machine Design and Research, **vol**. 33, no. 02, Apr. 2017, pp. 6-11.(In Chinese)

[10]. *Zarmehi F, Tavakoli A,* Construction of the matched multiple knot B-spline wavelets on a bounded interval[J], International Journal of Computer Mathematics, **vol**. 92, no. 8, Oct. 2014, pp. 1688-1714.

[11]. *Jiang Y, Li Y,* The research of the approximate algorithm based on cubic B-spline curves[C], 2012 Fifth International Conference on Information and Computing Science. IEEE, July 2012, pp. 23-26.

[12]. *Zhao X, Zhang C, Xu L, et al,* IGA-based point cloud fitting using B-spline surfaces for reverse engineering[J], Information Sciences, **vol**. 245, Oct. 2013, pp. 276-289.

[13]. *Wu Y R, Fan C W,* Mathematical modeling for screw rotor form grinding on vertical multi-axis computerized numerical control form grinder[J]. Journal of Manufacturing Science and Engineering, **vol**. 135, no. 5, Oct. 2013, pp. 051020(13 pages).

[14] *Shen Z H, Yao B, Chen B Q, et al,* A novel rotor profile error tracing and compensation strategy for high precision machining of screw rotor based on trial cutting of limited samples[J], Shock and Vibration, **vol**. 2015, 2015.

[15] *Shen Z, Yao B, Teng W, et al*. Generating grinding profile between screw rotor and forming tool by digital graphic scanning (DGS) method[J]. International Journal of Precision Engineering and Manufacturing, vol. 17, no. 1, Jan. 2016, pp.35-41.